Aronne Merrelli
Mark Smalley

Independent Lab: General Circulation with a Simulated β-plane

Abstract

A rotating tank with a conical insert is used to simulate a mid-latitude β -plane. Rossby waves are observed to propagate slower than the mean flow and to the East in the tank's rotating frame of reference. We show a good agreement between the theory and experiment for the difference in the translational speed of the eddies and the speed of the mean flow. Instability in the tank is seen to be increasingly sensitive to rotation speed than in an earlier general circulation experiment with a flat tank bottom. By comparing our situation to a 300mbar northern hemisphere projection, we see that the waves we observe in the tank are strong analogs to the mid-latitude jet stream.

Introduction

In Lab 2: General Circulation, we observed a rotating tank's response to a meridional temperature gradient on an f-plane. For this lab, we seek to observe the effect of a β-plane on the general circulation. The most notable result of including a β-plane on the equations of motion is a mid-latitude Rossby wave. To observe a mid-latitude Rossby wave, we must introduce a tank bottom insert such that the slope creates an effective β. The experimental setup's ratio of the perturbation potential vorticity to the mean potential vorticity should be similar to the same ratio seen in the mid-latitudes. To calculate this ratio, we use the linearized shallow water potential vorticity q.

$$q = \frac{f_o + \beta y + \zeta}{H} = \bar{q} + q' \tag{1}$$

Here, f_o is the initial planetary vorticity, βy is the first-order correction to the planetary vorticity, ζ is the relative vorticity, and H is the depth of the fluid. The mean potential vorticity for the mid-latitude jet can be calculated as follows.

$$\bar{q} \approx \frac{f_o}{H} \approx \frac{10^{-4}\,\mathrm{sec}^{-1}}{10km} = 10^{-5}\,\frac{1}{km \cdot \mathrm{sec}} \tag{2}$$

Likewise, the perturbation potential vorticity for the same mid-latitude jet is estimated using observed typical values.

$$q' \approx \frac{\beta y}{H} \approx \frac{10^{-8}(km^{-1}\,\mathrm{sec}^{-1})}{10km} = 10^{-6}\,\frac{1}{km \cdot \mathrm{sec}} \tag{3}$$

The ratio of the perturbation potential vorticity to the mean potential vorticity is then found to be $q'/\bar{q} = 0.1$. The relative vorticity ζ was left out of the calculation because it is many orders of magnitude smaller than f_o and βy.

To apply this potential vorticity ratio to our tank, we slightly modify the potential vorticity equation so it matches our experimental setup. There is no β in the tank, so it is set

to zero. Because we are introducing a sloping bottom to the tank, the depth H is no longer constant, and we must introduce an αy term where α is the slope and y is a meridional distance from the outer edge of the tank insert. An upward slope towards the center of the tank will decrease the depth, so the αy term is subtracted from H:

$$q_{setup} = \frac{f_o + \beta y + \zeta}{H - \alpha y} \approx \frac{1}{H}(f_o + \zeta)\left(1 + \frac{\alpha y}{H}\right) = \bar{q}_{setup} + q'_{setup} \quad (4)$$

While there is no real β in the experimental setup, there is what can be seen as an effective β_{eff}. The equation for the effective β_{eff} is shown below. A positive slope will give the same sign for β_{eff} as the actual midlatitude β in the Northern Hemisphere.

$$\beta_{eff} = \alpha \frac{f_o + \zeta}{H} \quad (5)$$

Separating the $\bar{q}_{setup}$ and q'_{setup}, we can multiply $\bar{q}_{setup}$ by the $q'/\bar{q} = 0.1$ ratio found earlier for the mid-latitude jet stream and solve for the insert slope $\alpha = \tan(\theta)$. We then see that in order to observe effects similar to those of the mid-latitude Rossby wave in the jet stream, we need a slope angle of about $\theta = 6°$.

The dispersion relation for mid-latitude Rossby waves divided by the zonal wavenumber k gives the zonal phase speed and is shown in the following equation.

$$c - \bar{u} = -\frac{\beta}{k^2} \quad (6)$$

The phase speed c minus the mean wind is equal to β divided by the zonal wavenumber k squared. The dispersion relation is derived from the horizontal momentum equations and the conservation of potential vorticity with an assumed exponential solution to the wave equation.

Methods

In order to create an analog of the beta plane in the rotating tank, we need to create a meridional slope at the bottom of the tank. The meridional axis in tank with the cylindrical insert points radially inward. A positive β effect thus corresponds to an upward slope toward the rotational axis of the tank; the tank floor must therefore have a conical shape. Simply changing to a conical shape at the tank floor still requires some mechanism for exciting waves in the tank, in order to investigate Rossby wave analogs; we decided the simplest way to create perturbations was to use the ice bucket in the center of the tank to create temperature gradients. The resulting setup is very similar to the standard tank experiment to create Hadley cell-like overturning circulations and thermal wind. In the Hadley cell experiment, a cylindrical insert is used to convert the square rotating tank into a circularly symmetric one. A circular metal bucket is placed at the center of the tank, and filled with ice, to create a forcing in the tank through temperature gradients. Figure 1 shows a cross section through the tank setup for the Hadley cell, along with the modification to add the slope at the bottom.

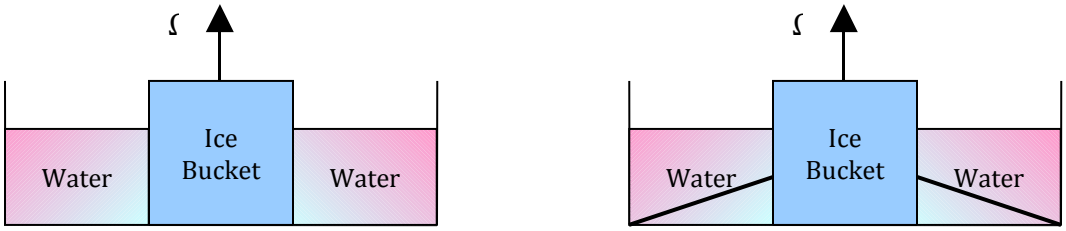

Figure 1. Schematic cross sections of the rotating tank, for the standard Hadley circulation analog (left), and the new setup with a sloping bottom to produce an effective β plane in the tank (right). The colors show the rough temperature gradient produced by the central cold source.

To simplify the construction of the sloping insert, we decided against constructing a watertight insert or attempting to make an entirely new tank with a conical bottom. A watertight insert would need to support the substantial water mass when the tank is filled. By allowing water to fill the space underneath the sloping insert, it does not need to be constructed out of very rigid materials, since it only needs to resist the force of the slow (few cm/s) currents generated within the tank. To make room for the ice bucket, the center of the conical insert must be removed. The final shape is a sloped annulus, similar to a funnel, but with a very shallow angle, and large central opening. Figure 2 shows a top and side view of the sloping insert (right half of figure).

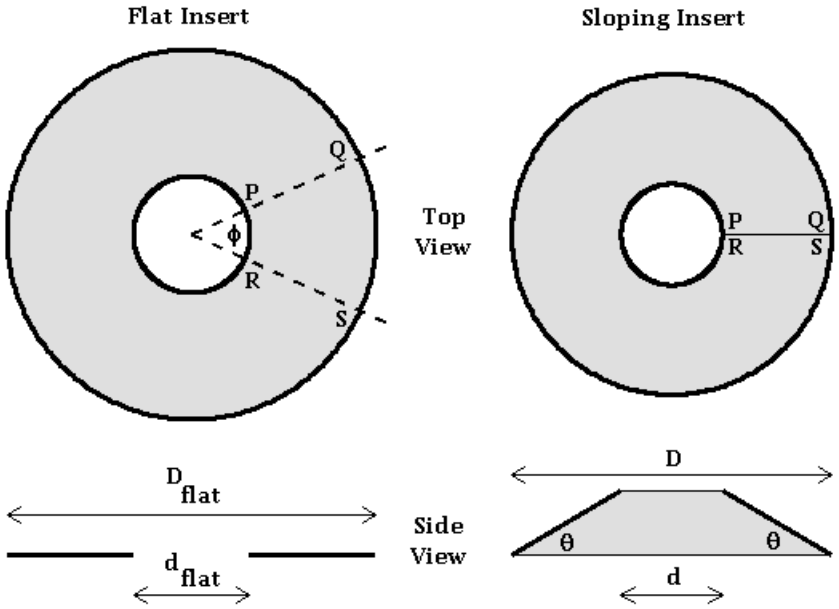

Figure 2. Schematic drawing showing the creation of the sloping insert. The insert is cut from a flat poster board (left side). After the wedge is removed the edges are rejoined, which bends the flat sheet into a cone (right side) with the diameters that match the ice bucket and cylindrical tank insert (d and D, respectively). The figure is drawn to scale, with a larger slope angle (30°) to more clearly show the slope.

Since the insert does not need to support the weight of the water above it, we

decided to construct it out of laminated poster board. The poster board can be easily cut and bent into the conical shape. First, a C-shaped piece of poster board is cut from the flat sheet (see left half of Figure 2). The C-Shape is then laminated to make the paper water resistant. The C-shape is then bent into the conical shape the two ends are fastened. The exact dimensions of the C-shape are related to the tank diameter and slope angle as follows. The end product is a cone with outer diameter D, which must match the diameter of the cylindrical insert in the tank; and an inner diameter of d, matching the diameter of the ice bucket. The cone makes an angle of θ inward from the outer diameter (see Figure 2, side view at bottom right). The diameters of the C-shape on the flat poster board (d_{flat}, D_{flat}) are related to the final diameters by the cosine of the slope angle

$$\cos(\theta) = \frac{d}{d_{flat}} = \frac{D}{D_{flat}} \tag{7}$$

The size of the wedge that must be removed is also related to the slope angle. This can be derived by noting that the arc lengths of the inner and outer edges of the C-shape must match the circumference of the ice bucket and the cylindrical tank insert:

$$\begin{aligned} s_{outer} &= (2\pi - \phi_{outer})\frac{1}{2}D_{flat} = \pi D \Rightarrow \phi_{outer} = \left(2\pi - 2\pi\frac{D}{D_{flat}}\right) = 2\pi(1-\cos(\theta)) \\ s_{inner} &= (2\pi - \phi_{inner})\frac{1}{2}d_{flat} = \pi d \Rightarrow \phi_{inner} = \left(2\pi - 2\pi\frac{d}{d_{flat}}\right) = 2\pi(1-\cos(\theta)) \end{aligned} \tag{8}$$

Thus, the wedge angle is directly related to the slope angle, and it is equal at the inner and outer edges. Once the wedge is removed, the paper is bent into the cone shape and the two sides are reattached at a joint between the opposing ends (the line segments PQ and RS in Figure 2).

Since the sloping insert is not a sturdy design, we set up the experiment by first filling the tank to the desired water depth, and then add the empty ice bucket and the sloping insert. The cylindrical insert is added last, in order to make sure the outer edge of the slope is pinned down at the bottom of the tank.

We designed inserts for angles of 5° and 15°. We had some difficulty getting the laminated poster board to bend into exactly the correct shape. First, the lamination adds a few extra millimeters around each edge. The small extra width was acceptable around the outer edge, but not around the inner edge bordering the ice bucket. In this case, the laminate was trimmed all the way back to the poster edge, and then clear plastic tape was used to reseal the laminate in order to keep the poster dry. The resulting C-shape turned out to be slightly too long when we curved it into shape, so there was some overlap at the joint. The other issue is keeping the slope constant around the entire circumference. Because of the junction between the two flat edges, the bending strength of the insert is different at the junction. Since we had to overlap the poster slightly, the insert did not bend as easily here, so the slope at the joint is somewhat lower than average. The slope at the opposite side is correspondingly larger than average. The end result for the sloping insert

designed for 15° was a slope in the range 15-20 degrees, varying according to the azimuthal position (e.g., the analog to the zonal coordinate in the atmosphere). We did not run an experiment with the 5 degree sloping insert, since the fitting problems were more severe. The wedge size for the 5 degree slope is very small, making the insert much more difficult to handle.

Experiments

Four experiments were run with the 15-20 degree sloping insert. The experimental setup was the same in each case, aside from the tank rotation rate. The procedure for each setup was to first fill the tank to a depth of 12 cm, then add the sloping insert, empty ice bucket, and cylindrical insert (in that order). The tank's motor was then set to the desired rotation speed, and the tank was allowed to settle for about 15-20 minutes to allow time for solid body rotation to be reached. At this time, ice and cold water was added to the ice bucket. After several minutes to allow the tank to adjust to the new flow regime, we added dye and surface tracers to characterize the fluid flows. The flows persist for as long as the ice has not fully melted, which is usually about 15-20 minutes.

When the Hadley-cell experiment was performed in a previous lab session, the tank rotation rate was set to a very slow speed (slightly less than 1 rpm) in order to produce the symmetric overturning circulation. The transition to eddy dominated circulations occurs at a very slow speed (1-2 rpm). Therefore, we decided to run experiments with the rotation speed set to 2.5, 5, and 10 rpm, in order to investigate different flow regimes.

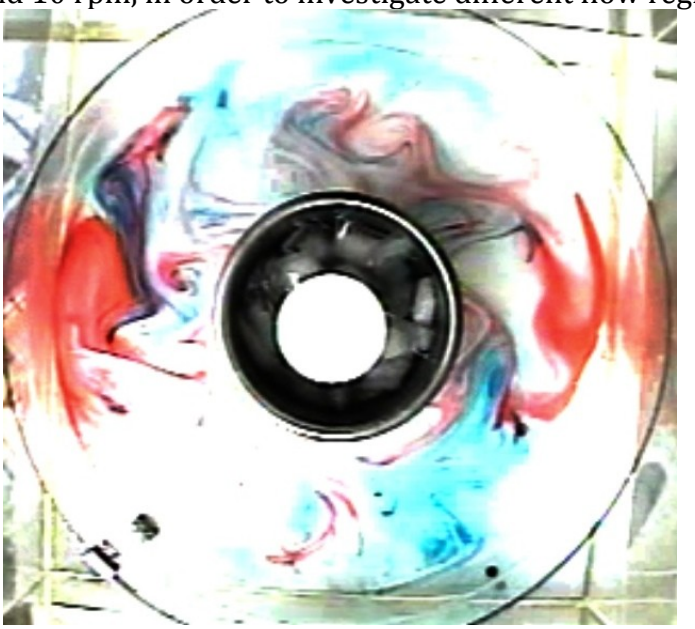

Figure 3. Eddies observed for the fast rotation (10 rpm) case.

The slow rotation experiment had a measured rotation speed of 2.6 rpm. In this case, an unexpected symmetric circulation was observed. Since the goal of this project was to observe wave patterns in the eddy regime, this slow rotation speed was not investigated further. The fast rotation speed (10 rpm) produced highly chaotic eddies. The lateral eddy sizes were quite small (perhaps a few cm), as shown in Figure 3. Furthermore, the vertical distribution showed eddy patterns, indicating three dimensional vortex interactions and a

breakdown of the Taylor columns. This experiment was not investigated further since the breakdown of the two dimensional symmetry implies the flow in the tank no longer is a useful analog of the atmospheric circulation. The middle rotation speed (5 rpm) produced eddy circulations, along with jet flows, and Rossby wave like patterns. An example of the observed eddy circulation is shown in Figure 4. This experiment was performed twice with the tank camera running, with flow tracers in place to measure flow speed. A third experiment was run as a demonstration but no quantitative data was collected. The analysis and discussion of the experiment is based entirely on these experiments.

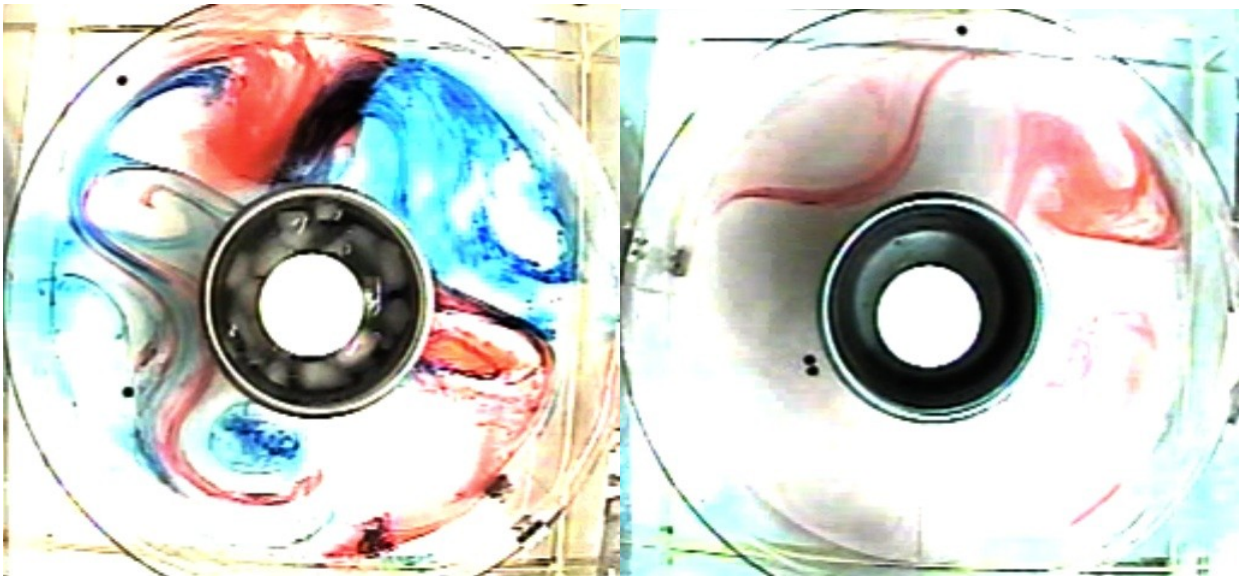

Figure 4. "Four wave" eddy pattern observed at 5 rpm (left). Dye streak indicating jet flow at 5 rpm (right). The two pictures were taken at much different times, so the eddies have propagated around the tank.

Figure 4 shows the eddy circulation for one of the 5 rpm experiments. The flow shows a clear "four-wave" pattern, with four large eddies, roughly 10 cm in diameter, spaced evenly around the zonal dimension. The flow around the outer ("southern") edge of each eddy shows a jet-like flow. Figure 4 also shows a dye track within the jet. In the two main experiments, the circulation formed a strong four wave pattern very quickly. In the third demonstration experiment, the initial flow was much more irregular. A weaker four-wave pattern was eventually observed much later in the experiment.

The flow patterns were analyzed using sections of the digitized video stream from the co-rotating camera. Since the flow speeds are still quite slow, the videos were saved to a DVD and then replayed at triple normal speed while digitizing the video on the computer. The triple speed allows for much smoother visualizations of the flow without needing to "fast forward" the movie on the computer. Long tracks using particle tracking software were obtained for two particular surface tracers, one tracer following the cyclic flow inside the eddy, and another tracer following the fast jet flow. A segment of the dye track inside the jet was tracked manually by noting the position of the front edge of the dye track as it progressed around the tank. Finally, an estimate of the speed of the entire eddy was manually obtained by noting the angular position of the eddy cores through time. The angular position around the tank is essentially a longitude measurement, so by assuming a radius (e.g., a latitude) equal to the middle of the tank annulus, the angular speed can be

converted to a linear speed in cm / s. Figure 5 shows the angular measurement of one particular eddy as it circulates in a counterclockwise (cyclonic) path around the center of rotation.

Figure 5. Speed estimation for eddies. Each eddy has an angular velocity, estimated by the green line segments. Multiplying the angular speed by 20 cm yields an estimate of the eddy linear speed.

Data Analysis

The three extracted tracks are shown in Figure 6, along with the corresponding calculated speeds. The calculated speeds are the magnitudes of the velocity vector at each point, since the displacements were not decomposed into vector components (e.g., the zonal and meridional speeds were not estimated). The eddy speeds were computed for each of the four eddies, by measuring the displacement between two widely separated times in the recorded movie, when the dye was clearly defining the eddy perimeters. The summary of the different speed measurements is shown in Table 1.

Table 1. Estimated speeds of various flow tracers.

Flow component	Vertical position	Estimated Speed [mm / s]
Particle tracer in jet	Surface ($z = H$)	10-20
Particle tracer in eddy	Surface ($z = H$)	5-15
Dye track in jet	interior ($z \sim H/2$)	3-5
Eddy	Integrated depth ($z \sim 0 \rightarrow H$)	1.5-3

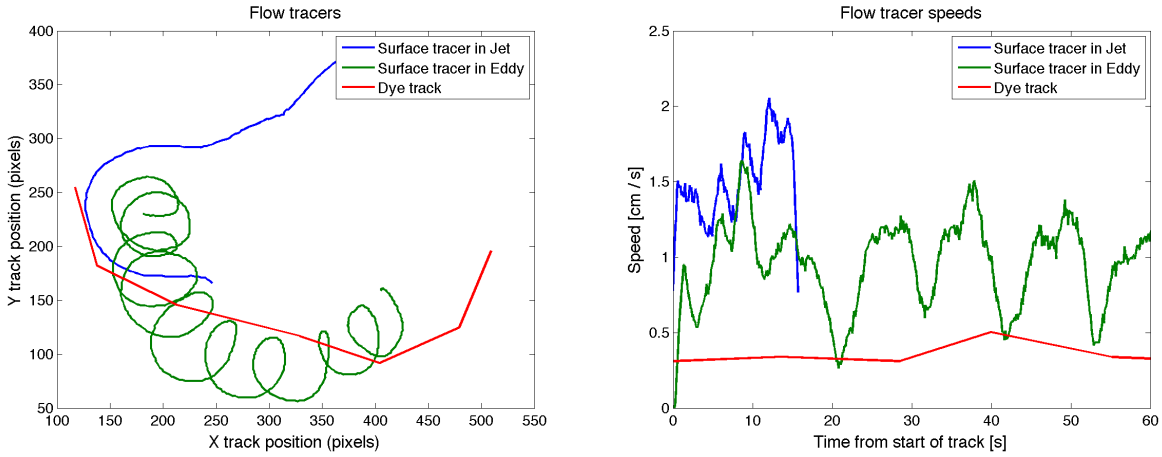

Figure 6. Tracked positions of the various fluid flow tracers (left), and the computed speeds (right).

Plugging in experimental values for the slope, zonal wavenumber, and β_{eff} into the Rossby wave phase speed equation, we see that the difference between the Rossby phase speed and the mean wind is predicted to be about 3mm/sec.

$$c - \overline{u} = -\frac{0.306\left(\frac{\pi}{3}\frac{rad}{sec}\right)(12cm)^{-1}}{\left(0.28cm^{-1}\right)^2} \approx -3mm/sec$$

During the experiment, we note that the observed difference between the phase speed of the eddies and the mean wind in the interior of the fluid is between 1.5mm/sec and 2.0mm/sec. This is a good agreement, considering the large uncertainty of the speed measurements.

A qualitative comparison between the observed eddy circulation and the real atmosphere circulation in the mid-latitude shows strong similarities. Figure 7 shows a 300mb geopotential field (contours) and wind speed (colors), from a Numerical Weather Prediction model, with a display grid centered on the North Pole. The particular field is from analysis, so the NWP model has only assimilated current observational data, and has not predicted future time steps. The high jet winds are located around the southern edges of eddy like features in the geopotential height, in the same pattern as observed in the tank experiment. In addition, the jet winds have a higher zonal (eastward) speed than the eddies, in the same manner as observed in the rotating tank experiment. Both flow patterns are within rough agreement to the prediction from the Rossby wave dispersion relation (equation 6).

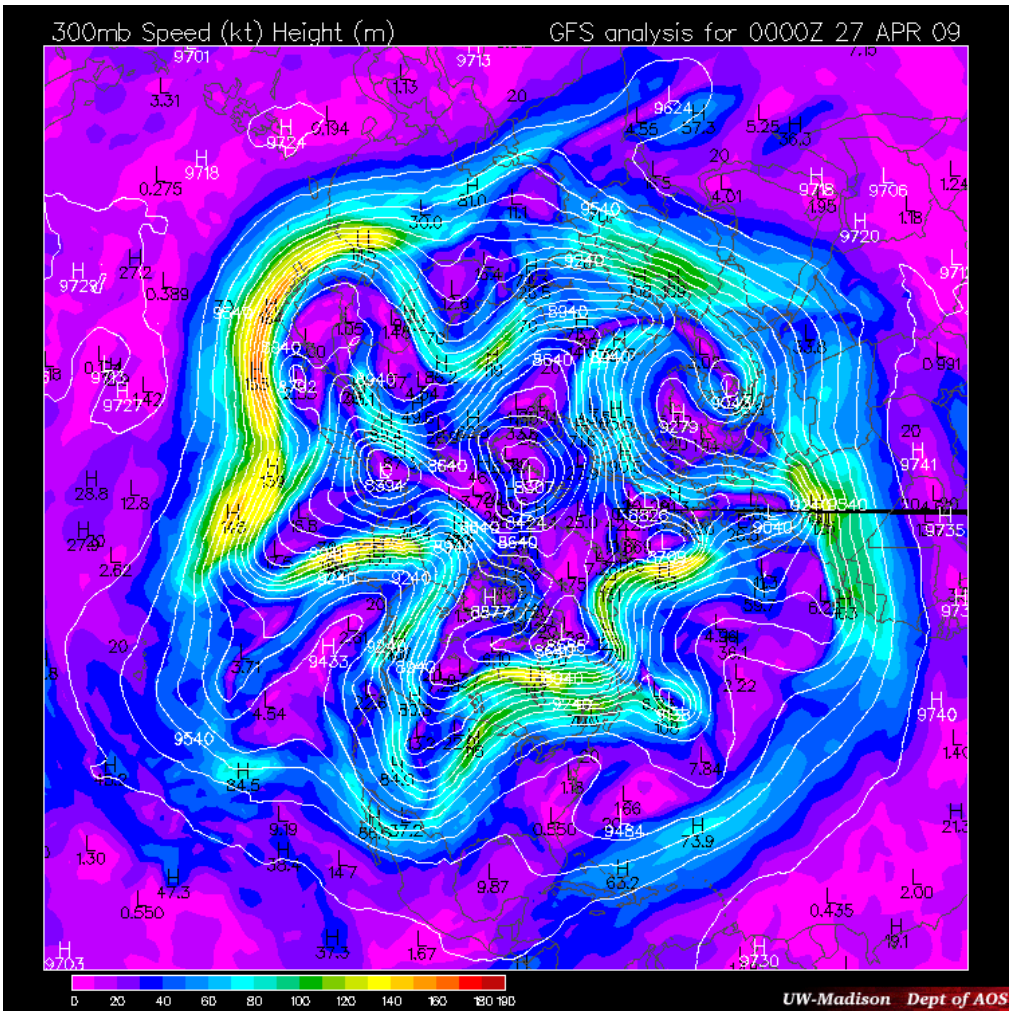

Figure 7. 300 mb geopotential heights and wind speeds from NCEP GFS model analysis.

Discussion

We observe waves in the rotating tank that closely resemble the mid-latitude jet stream Rossby wave when the rotation rate is about 5rpm and the insert angle is about 17°. We see that the translational speed of the eddy cores is an analog to the phase speed, and the speed of the dye is representative of the Rossby wave mean zonal flow. The four-wave eddies propagate eastward in the tank, but westward relative to the mean flow. From these visible connections to the real-world situation, we conclude that a cone-shaped tank bottom does produce an effective β-plane that results in a Rossby wave-like flow pattern.

The effective β resulting from the tank bottom insert introduces a more complicated and more sensitive flow pattern than what was observed during the general circulation lab. When the tank's rotation rate was increased to 10rpm, the rigid vertical structure of the flow was all but entirely lost to three-dimensional eddy flows and the four-wave pattern broke down into a multitude of random eddies. During the general circulation lab, we observed a Hadley regime until about 1-2 rpm, then the flow turned turbulent with fairly stationary eddies (in the rotating frame) and stayed that way until about 15rpm. With an artificial β-plane, the Hadley circulation was still observed at 2.5rpm. The Rossby wave

circulation was observed at 5rpm, but is not present at 10rpm.

Future work could involve an experiment dealing with different slopes of the tank insert. The more realistic direction for the change in slope to be is towards a smaller angle, perhaps around 7 or 8 degrees. A change in the slope will change the value of β_{eff} and potentially change the number of eddies and propagation and eddy rotation speeds. Future experimenters might also prefer to cut their paper a bit shy of the intended width of the insert, because lamination of the paper adds a small amount of material at the edges that if cut off, allows water to creep between the laminate layers and soak the paper. Other variants of this experiment could involve altering the tank's rotation rate. This would also affect the β_{eff}, which would in turn affect q', but it would also affect the mean potential vorticity.